Homogeneous Hydrophobic–Hydrophilic Surface Patterns Enhance Permeation of Nanoparticles through Lipid Membranes

ARTICLE *in* JOURNAL OF PHYSICAL CHEMISTRY LETTERS · MAY 2013

Impact Factor: 7.46 · DOI: 10.1021/jz400679z

3 AUTHORS, INCLUDING:

Paraskevi Gkeka
Biomedical Research Foundation
18 PUBLICATIONS **113** CITATIONS
SEE PROFILE

Lev Sarkisov
The University of Edinburgh
60 PUBLICATIONS **1,624** CITATIONS
SEE PROFILE

THE JOURNAL OF PHYSICAL CHEMISTRY Letters

Letter

pubs.acs.org/JPCL

Homogeneous Hydrophobic–Hydrophilic Surface Patterns Enhance Permeation of Nanoparticles through Lipid Membranes

Paraskevi Gkeka,[†,§] Lev Sarkisov,[†] and Panagiotis Angelikopoulos*[,‡]

[†]Institute for Materials and Processes, School of Engineering, University of Edinburgh, Edinburgh, United Kingdom

[‡]Computational Science and Engineering Laboratory, Universitätstrasse 6, ETH Zurich, CH-8092, Switzerland

Supporting Information

ABSTRACT: We employ coarse-grained molecular dynamics simulations to understand why certain interaction patterns on the surface of a nanoparticle promote its translocation through a lipid membrane. We demonstrate that switching from a random, heterogeneous distribution of hydrophobic and hydrophilic areas on the surface of a nanoparticle to even, homogeneous patterns substantially flattens the translocation free-energy profile and dramatically enhances permeation. We then proceed to construct a more detailed coarse-grained model of a nanoparticle with flexible hydrophobic and hydrophilic ligands arranged into striped domains. Molecular dynamics simulations of these nanoparticles show that the terminal groups of the ligands tend to arrange themselves into homogeneous patterns, despite the underlying striped domains. These observations are linked to recent experimental studies.

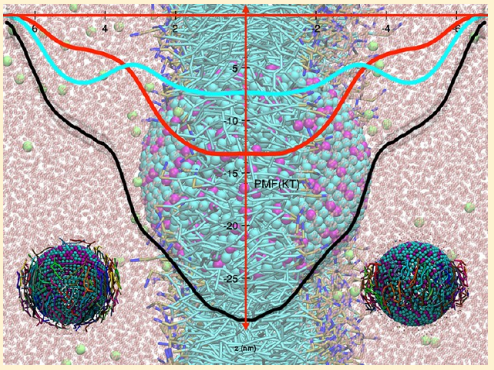

SECTION: Physical Processes in Nanomaterials and Nanostructures

In the past decade, nanoparticles (NPs) have emerged as a promising new class of drug and gene delivery vectors as well as agents for targeted destruction of cancer cells.[1−5] However, these engineered nanomaterials may also have some unintentional, adverse properties. Ideally, NPs should be able to enter the target cell without getting trapped in endosomes, as this would prevent the delivery of the drug (or gene) of interest, leading to drug isolation and eventual decay. Concurrently, NPs should be biocompatible and not toxic. There has been a substantial research effort to understand how NP properties, such as their material, size, shape, surface chemistry, and charge, influence their interactions with cell membranes.[2,4−26] A detailed description of these interactions on molecular level is required to be able to design bespoke NPs with programmable and controlled membrane translocation mechanisms.

Among intriguing recent contributions in this field is a series of studies by Stellacci and coworkers.[27−29] In the original study, the authors considered gold NPs, coated with hydrophobic (octanethiol, OT) and hydrophilic (mercaptopropionic acid, MPA) ligands. The authors argued that depending on the composition the ligands self-assemble on the NP surface into ordered, well-defined stripes. Translocation of Striped NPs through the cellular membranes has been investigated in consequent in vivo studies on fibroblast cells.[28,29] Gold NPs of 4.3 to 4.9 nm core diameter with surface functionalized to be uniformly hydrophilic required endocytotic pathway of translocation, whereas particles featuring regular, striped patterns of hydrophobic (OT) and hydrophilic (11-mercapto-1-undecanesulphonate, MUS) domains translocated via both endocytotic and some direct mechanism not requiring receptors or energy.

The study of Stellacci and coworkers suggests that the NP surface pattern can be used as a simple tuning parameter to drastically change the mechanism of its internalization by a cell, with this claim attracting substantial interest in the research community. Recently, an alternative interpretation of the original study has emerged, questioning the existence of striped domains and the mode of their interaction with cell membranes.[5,30] It is, therefore, crucial to develop understanding of these systems at the molecular level.

Several recent simulation studies focused specifically on the actual effect of hydrophobic and hydrophilic patterns on the ability of a nanoscale object to translocate through a lipid membrane. Theoretical and simulation studies typically consider simplified systems compared with the in vivo processes. They model membranes as lipid bilayers, made of one type of lipids and devoid of membrane proteins, cholesterol, and other vital components of the cell membrane. In vivo, the medium in the vicinity of the membrane also contains proteins and other species that would tend to form the so-called corona around any nano-object,[29] influencing their interaction with the aforementioned species. However, a simplified representation of the system in simulation studies is important not only for a better computational efficiency but also as a way to systematically decouple a number of complex effects. For example, Pogodin and Baulin employed a self-consistent mean-field approach to investigate the translocation

Received: March 28, 2013
Accepted: May 17, 2013

   dx.doi.org/10.1021/jz400679z | J. Phys. Chem. Lett. 2013, 4, 1907−1912

of patterned nanotubes through a model lipid bilayer.[31] The patterned nanotubes featured alternating hydrophobic and hydrophilic 1 nm thick rings on their surface. Such nanotubes, when vertically inserted in the bilayer, have at any given position an equal number of favorable domain contacts and unfavorable interactions. It was shown that this domain distribution leads to flat and low free-energy profiles of nanotube insertion in the bilayer and interestingly this phenomenon was not reproduced for nanotubes featuring uniform surfaces. Flat free-energy profiles were observed only for thin nanotubes of 1 nm in diameter, whereas for wider nanotubes (2.43 nm) barriers still remained substantial. It seems that this enthalpic argument can be used to construct a plausible explanation of the outcomes from Stellacci and coworkers, but important differences between thin nanotubes and NPs must be recognized. Notably, the study of Pogodin and Baulin considered only fixed vertical orientation of nanotubes with respect to the bilayer plane. In this case, lipid molecules are aligned along the nanotube, the lipid bilayer is not substantially perturbed, and it can be viewed as a system of two hydrophilic slabs on the outside of the layer and a hydrophobic slab in the center. Placing an NP with a diameter bigger than the bilayer thickness within the bilayer causes substantial perturbation of its structure, and regardless of the NP surface patterning, its spherical shape prevents a similar alignment of the lipid molecules to that observed for the vertically inserted nanotubes.[32] A system more closely resembling the NPs of Stellacci and coworkers has been recently considered by Li et al.[23] Using dissipative particle dynamics (DPD), they investigated NPs of diameter equal to about 4/5 of the bilayer thickness, featuring striped and random distribution of hydrophilic and hydrophobic groups. The authors observed that the Striped NP experiences a significantly lower free-energy barrier compared with the NP with the same surface group composition but with a random distribution of these groups. They associated this effect with the entropy loss of the Striped NP due to its restrained rotation in the bilayer and accounted this mechanism responsible for the experimental observation by Stellacci and coworkers.

We offer an alternative and simple explanation of why regular patterns of surface hydrophobicity and hydrophilicity, similar to the ones used by Stellacci and coworkers, enhance NP propensity to translocate through a lipid membrane. We employ coarse-grained molecular dynamics (CGMD) simulations following the methodology described in our previous work.[32,33] We consider a system of a preformed lipid bilayer, surrounded by water, and an NP of ∼6 nm in diameter initially placed in the water phase. The energetics of all of the components of the system are described using the MARTINI CG force field.[34] The propensity of the NP to cross the lipid bilayer is characterized by the potential of mean force (PMF) along the translocation path. Deep minima in the potential profile mark the locations where the NP tends to get trapped, whereas a shallow and uniform PMF corresponds to a relatively easy, barrier-free translocation process. These PMFs are generated using the standard combination of the Umbrella Sampling technique and Weighted Histogram Analysis Method (WHAM).[35−37] More information about our system set up and simulation parameters can be found in the Supporting Information (SI).

Using a catalogue of standard CG beads from the MARTINI force field, NPs with various hydrophobic and hydrophilic patterns on their surface can be constructed. To a significant extent, this investigation has been prompted by previous studies and our own observations, suggesting that predominantly hydrophobic NPs with a random distribution of hydrophobic and hydrophilic CG beads on their surface tend to get trapped in the core of the lipid bilayer. For example, consider an NP with a 6 nm diameter, similar to those studied by Stellacci and coworkers. The chemistry of the MUS sulfonate ionic groups is represented with MARTINI Qa negatively (−1) charged beads, whereas hydrophobic ligands are represented with MARTINI C1 particles. There are a total of 274 hydrophilic and 834 hydrophobic CG beads randomly placed on the surface of the NP to reflect the composition of one of the systems explored by Stellacci and coworkers (labeled 34-66 OT in the original study[28]). The PMF for this heterogeneous random pattern features a relative potential minimum of ∼28 kT compared with the starting position in the water phase (Figure 1, black).

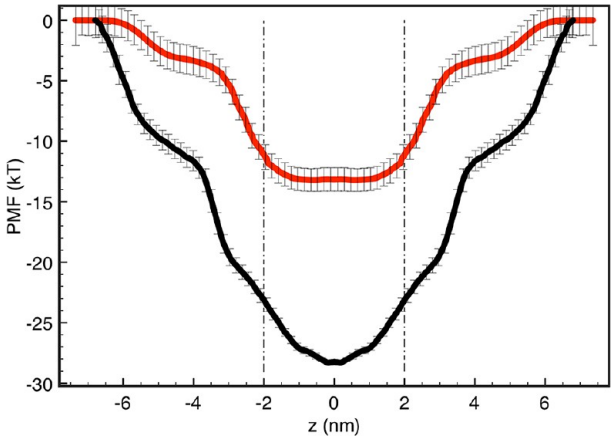

Figure 1. PMFs for the random (black) and homogeneous NP (red). Dashed lines indicate the position of the glycerine groups in the lipid bilayer. The errors have been calculated using the standard bootstrapping technique.

We acknowledge here that the PMF is not fully leveled out, which is not surprising, given the size of the NP. Molecular visualization of the different states of the system during the translocation process reveals that as the NP moves along the translocation path, the structure of the lipid bilayer substantially rearranges itself to accommodate it, with some lipid molecules adhering to the larger hydrophobic areas on the surface of the NP (Figure 2).

Suppose we maintain the same proportion of hydrophilic and hydrophobic CG beads (274:834) as for the NP shown in Figure 2. Is it possible to design a pattern that would substantially reduce the free energy minimum in the PMF, and thus improve the translocation characteristics? Observations summarized above suggest that one way to achieve this is by avoiding large hydrophobic patches on the surface of the NP, at least as much as possible within a given composition.

To test this hypothesis, we design an NP with the same number of hydrophobic and hydrophilic CG beads on the surface as before but with these beads arranged in a homogeneous pattern via a variation of the golden spiral algorithm promoting the hydrophilic groups to be uniformly and equidistantly separated from each other (more details can be found in the SI). To characterize the distribution of hydrophobic regions, we employ Voronoi tessellation analysis on a sphere, with the hydrophilic groups serving as seeds in this

dx.doi.org/10.1021/jz400679z | J. Phys. Chem. Lett. 2013, 4, 1907−1912

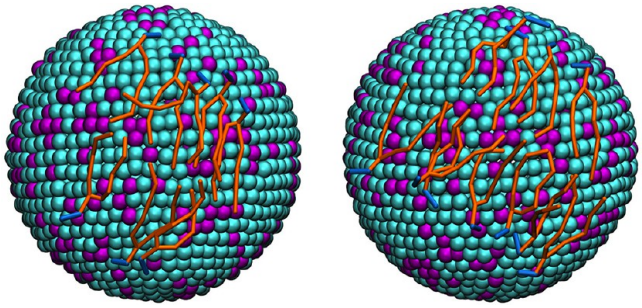

Figure 2. Snapshots from the Umbrella Sampling simulations showing examples of the self-assembly of lipids close to large hydrophobic areas on the surface of the random NP. The snapshots correspond to the NP located at the center of the lipid bilayer. Colors: hydrophobic CG particles = cyan, hydrophilic CG particles = magenta, lipid tails = orange, and lipid heads = blue.

process.[38] Voronoi diagrams for the original NP with a random, heterogeneous pattern and the designed NP with the homogeneous pattern (henceforth referred to as homogeneous NP) are shown in Figure 3. This visualization highlights the

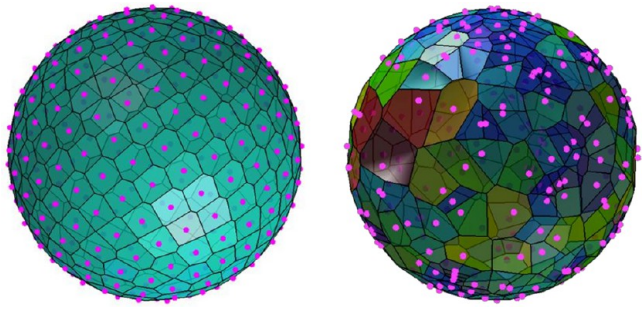

Figure 3. Spherical Voronoi diagram for a homogeneous (left) and a random (right) distribution of 274 sites on a sphere of a 6 nm diameter. Colors indicate cell area from zero (deep blue) to 1.5 nm^2 (dark red).

differences between the two patterns, with the homogeneous surface looking ordered and regular. The size of a Voronoi cell in this construction corresponds to the size of the hydrophobic area surrounding a particular hydrophilic CG particle. Figure 4 shows area distributions of hydrophobic regions, as defined by the Voronoi tessellas. Indeed, these distributions are strikingly different for the two NPs, with the heterogeneous random pattern leading to a broad area distribution and a long tail in the larger area domain, whereas the homogeneous pattern is associated with a well-defined, narrow peak size around 0.41 nm^2.

Figure 1 compares the PMFs for the two NPs, and the difference is remarkable. The free-energy minimum for the NP with the homogeneous pattern is more than two times smaller (−13 kT) than that for the NP with the random heterogeneous pattern (−28 kT). The PMF for the homogeneous NP also levels out at ∼6 nm away from the bilayer center, indicating that the effective interactions operate on a shorter range compared with the random NP. To understand how the difference in the two PMF profiles affects NP permeability (P), we use the approach of Berendsen et al.[39] following an inhomogeneous solubility−diffusion model, with permeability being a function of both the free energy of solvation difference

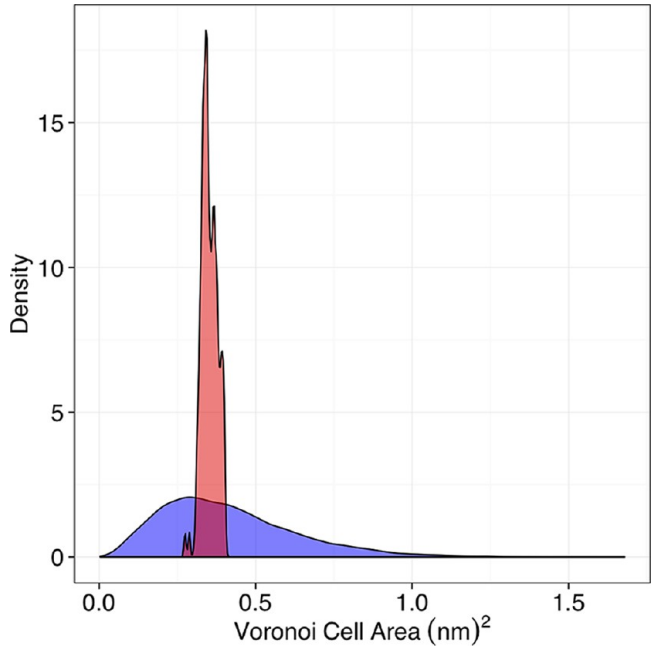

Figure 4. Area distributions of the Voronoi tessellation cells for random (blue) and homogeneous (red) NPs.

and the change of the NP vertical (z-dimension) diffusion coefficient D_z:

$$\frac{1}{P} = \int_{z_1}^{z_2} \frac{e^{\Delta G(z)/kT}}{D_z(z)}\, dz \tag{1}$$

and

$$D_z(z) = \frac{(RT)^2}{\int_0^\infty \langle \Delta F_{(z,t)} \Delta F_{(z,0)} \rangle\, dt} \tag{2}$$

where k is the Boltzmann constant, T is the temperature, $\Delta G(z)$ is the potential of mean force as a function of distance z between the center of the bilayer and the current position of the NP, and D_z is the local diffusion coefficient at this z position. The latter property is estimated using the force autocorrelation method eq 2[40] where ΔF is the force required to restrain the position of the NP during the creation of the potential of mean force profile $\Delta G(z)$. In eq 2, brackets denote ensemble averaging, R is the gas constant, and z is the perpendicular distance between the center of mass of the NP and the membrane at time t. The permeability coefficients according to this model are dominated by the exponential dependence of the free-energy transfer between the two states provided that the diffusion coefficient changes only within a single order of magnitude, as is the case here. Hence, even a small difference in the free energy becomes exponentially more important when it comes to the time required to enter or escape from the membrane. Here eq 1 is integrated from $z = 0$ (membrane center) until almost the bulk water region at $z =$ 6.8 nm. We estimate the ratio of the homogenous to random NP permeation coefficients to be $P_H/P_R \approx 5 \times 10^6$. These differences in the PMFs and permeabilities can be explained as follows: larger hydrophobic patches on the surface of the random NP provide favorable locations for lipid self-assembly effectively binding the NP within the bilayer. Interestingly, the self-assembled clusters of lipids on these patches are stable enough so that they are dragged along with the underlying

dx.doi.org/10.1021/jz400679z | J. Phys. Chem. Lett. 2013, 4, 1907−1912

patches as the NP rotates or moves through the bilayer (Figure 5, inset). One of the manifestations of this process is a strong

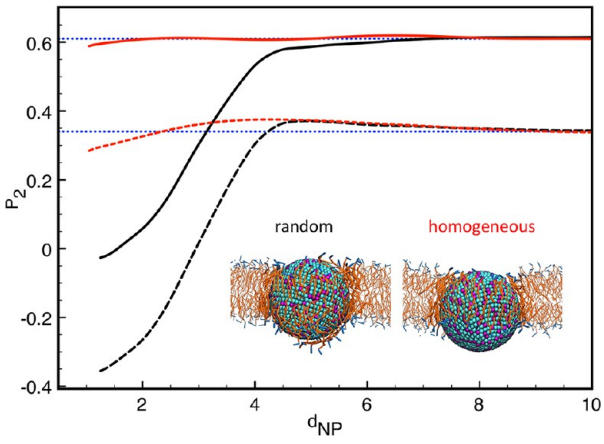

Figure 5. P_2^{NMR} (dashed) and $P_2^{(PO4\text{-}NC3)}$ (solid) order parameters for the random (black) and homogeneous (red) NPs as a function of distance to the NP surface (d_{NP}). Blue dotted lines indicate the model theoretical values acquired for an unperturbed bilayer. Inset: Visualization of the lipids arrangement around NPs with the color-coding as in Figure 1.

structural disorder of the lipid bilayer in the presence of the random NP. To characterize this disorder, we estimate two orientational lipid bond order parameters associated with both the hydrophobic tail groups P_2^{NMR} and headgroup $P_2^{(PO4\text{-}NC3)}$[41] (Figure 5, also see SI for more information). The random NP causes substantial deviation of these characteristics from the undisturbed bilayer properties, whereas the homogeneous NP leaves the bilayer almost intact by cumbering lipid aggregation on its surface.

This difference in the behavior of two considered NP patterns is not a chance event, associated with a particular selection of the systems. In the SI, we consider an extensive set of NPs and systematically demonstrate that reducing the size of hydrophobic domains (while maintaining the same surface composition) leads to a more shallow PMF profile. In addition to this, we examine the sensitivity of the observed picture to various simulation parameters, such as the time length of the simulations required to obtain reliable results.

We now make a speculative connection between the NP patterns considered in this article and the experimental results of Stellacci and coworkers. Homogeneous patterns similar to the one considered herein spontaneously emerge in systems featuring a distribution of discrete, freely moving charged sites on a spherical surface. This process is driven by repulsive interactions between the sites and their tendency to adopt an equidistant position from other charged sites. Finding an arrangement of these charges, which corresponds to the energy minimum of the system, is a classical Thomson problem.[42−44] Note that the organic molecules used as ligands by Stellacci and coworkers are essentially alkane chains with either 8 alkane groups (OT) or 11 alkane groups ending with a sulfonate ionic group (MUS). The molecules are flexible and can rearrange themselves on the surface of the NP. The difference in the length of the chains leads to the cross-section of the striped domains having a groove profile. Singh et al. proposed an entropic explanation for the formation of these domains: although two ligand species tend toward complete phase separation, interfaces between longer and shorter chains provide free volume for longer chains to move around; this leads to a gain in the conformational entropy, resulting from the existence of the stripes, sufficient to overcome energy penalties.[45] We argue that if the chains forming the stripes have enough freedom to explore the available free volume, then they form what resembles a homogeneous surface, despite the underlying striped pattern. To test this hypothesis, we construct a CG model of an NP, featuring ligand chains grouped in striped domains, as shown in Figure 6 (left). The structure this NP attains upon equilibration is shown in Figure 6 (center), whereas the Voronoi tessellation diagram of the final structure is shown in Figure 6 (right). The area distribution of the Voronoi tessellation cells for this system is shown in Figure S8 of the SI file. Although it is not a perfectly homogeneous pattern, the similarity of the diagram to that shown in Figure 3 is quite striking.

Naturally, it would be very interesting and important to understand the translocation process of a realistic NP model with flexible ligands as described above. We note here that this is a computationally challenging task requiring much longer

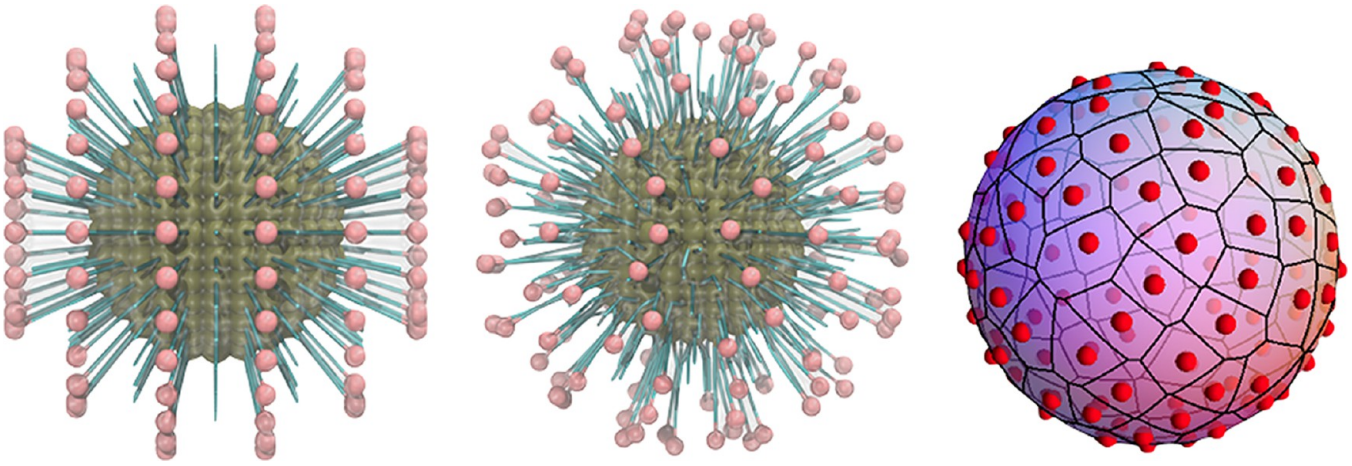

Figure 6. Coarse-grained representation of a "Striped" NP (left). The ligands are grafted to the hydrophilic core. The hydrophobic chains are presented as bonds, while negatively charged Qa beads are shown in pink. Typical structure of the "Striped" NP following equilibration with standard MD (center). Voronoi diagram on the sphere of the equilibrium structure (right).

dx.doi.org/10.1021/jz400679z | J. Phys. Chem. Lett. 2013, 4, 1907−1912

equilibration times to obtain a PMF with sufficient accuracy. Explicit representation of ligands also substantially expands the available parameter space (which now includes, for example, length of ligands, thickness of stripes, and so on) and a systematic consideration of many systems, as it has been done in the SI for the simplified smooth NPs, is unlikely to be computationally tractable for more detailed NP models. Also, in the present study, we have used a fixed level of NP hydrophobicity; studying the NP−membrane interactions and the effects observed in our present studies as a function of composition would be a natural extension of the present work.

Regardless of whether it is a simulated system or an actual experiment, it remains unclear to what extent NPs are able to preserve their patterns formed by flexible chains upon a contact with the lipid bilayer, and this will be a subject of further investigations. Hence, here we constrained ourselves to merely stating that within the synthetic protocol of Stellacci and coworkers homogeneous patterns are possible. According to our studies, if preserved, homogeneous patterns facilitate and enhance passive translocation of an NP through lipid membranes by preventing lipid aggregation on its surface. Furthermore, we envision that even in the case of the endocytotic pathway, Homogeneous NPs may disentangle more easily from endosome entrapment as opposed to random NPs that allow for lipid aggregation around them.

■ ASSOCIATED CONTENT

Supporting Information

CG model, simulation parameters, PMF and permeability calculations, algorithm of homogeneous patterns design, as well as different NP patterns that have been used in our work. This material is available free of charge via the Internet at http://pubs.acs.org.

■ AUTHOR INFORMATION

Corresponding Author

*E-mail: panagiotis.angelikopoulos@mavt.ethz.ch.

Present Address

[§]Paraskevi Gkeka: Biomedical Research Foundation, Academy of Athens, 4 Soranou Ephessiou, 11527, Athens, Greece.

Notes

The authors declare no competing financial interest.

■ REFERENCES

(1) Ferrari, M. Cancer Nanotechnology: Opportunities and Challenges. *Nat. Rev. Cancer* **2005**, *5*, 161−171.

(2) Jain, P. K.; El-Sayed, I. H.; El-Sayed, M. A. Au Nanoparticles Target Cancer. *Nano Today* **2007**, *2*, 18−29.

(3) Davis, M. E.; Chen, Z.; Shin, D. M. Nanoparticle Therapeutics: An Emerging Treatment Modality for Cancer. *Nat. Rev. Drug Discovery* **2008**, *7*, 771−782.

(4) Park, K.; Lee, S.; Kang, E.; Kim, K.; Choi, K.; Kwon, I. C. New Generation of Multifunctional Nanoparticles for Cancer Imaging and Therapy. *Adv. Funct. Mater.* **2009**, *19*, 1553−1566.

(5) Ding, H.-m.; Ma, Y.-q. Interactions between Janus Particles and Membranes. *Nanoscale* **2012**, *4*, 1116−1122.

(6) Lipowsky, R.; Dobereiner, H. G. Vesicles in Contact with Nanoparticles and Colloids. *Europhys. Lett.* **1998**, *43*, 219−225.

(7) Noguchi, H.; Takasu, M. Adhesion of Nanoparticles to Vesicles: A Brownian Dynamics Simulation. *Biophys. J.* **2002**, *83*, 299−308.

(8) Deserno, M. When Do Fluid Membranes Engulf Sticky Colloids? *J. Phys.: Condens. Matter* **2004**, *16*, S2061−S2070.

(9) Livadaru, L.; Kovalenko, A. Fundamental Mechanism of Translocation across Liquidlike Membranes: Toward Control over Nanoparticle Behavior. *Nano Lett.* **2006**, *6*, 78−83.

(10) Ginzburg, V. V.; Balijepalli, S. Modeling the Thermodynamics of the Interaction of Nanoparticles with Cell Membranes. *Nano Lett.* **2007**, *7*, 3716−3722.

(11) Qiao, R.; Roberts, A. P.; Mount, A. S.; Klaine, S. J.; Ke, P. C. Translocation of C-60 and Its Derivatives across a Lipid Bilayer. *Nano Lett.* **2007**, *7*, 614−619.

(12) Alexeev, A.; Uspal, W. E.; Balazs, A. C. Harnessing Janus Nanoparticles to Create Controllable Pores in Membranes. *ACS Nano* **2008**, *2*, 1117−1122.

(13) Bothun, G. Hydrophobic Silver Nanoparticles Trapped in Lipid Bilayers: Size Distribution, Bilayer Phase Behavior, and Optical Properties. *J. Nanobiotechnol.* **2008**, *6*, 13.

(14) Leroueil, P. R.; Berry, S. A.; Duthie, K.; Han, G.; Rotello, V. M.; McNerny, D. Q.; Baker, J. R.; Orr, B. G.; Holl, M. M. B. Wide Varieties of Cationic Nanoparticles Induce Defects in Supported Lipid Bilayers. *Nano Lett.* **2008**, *8*, 420−424.

(15) D'Rozario, R. S. G.; Wee, C. L.; Wallace, E. J.; Sansom, M. S. P. The Interaction of C-60 and Its Derivatives with a Lipid Bilayer Via Molecular Dynamics Simulations. *Nanotechnology* **2009**, *20*, 115102.

(16) Fiedler, S. L.; Violi, A. Simulation of Nanoparticle Permeation through a Lipid Membrane. *Biophys. J.* **2010**, *99*, 144−152.

(17) Schneemilch, M.; Quirke, N. Molecular Dynamics of Nanoparticle Translocation at Lipid Interfaces. *Mol. Simul.* **2010**, *36*, 831−835.

(18) Wallace, E. J., Sansom, M. S. P., Molecular Dynamics Studies of the Interactions between Carbon Nanotubes and Biomembranes. In *Molecular Simulations and Biomembranes: From Biophysics to Function*; Biggin, P. C., Sansom, M. S. P.P., Eds.; RSC: Cambridge, U.K., 2010; Vol. *20*, pp 287−305.

(19) Lin, X.; Li, Y.; Gu, N. Nanoparticle's Size Effect on Its Translocation across a Lipid Bilayer: A Molecular Dynamics Simulation. *J. Comput. Theor. Nanosci.* **2010**, *7*, 269−276.

(20) Lee, O.-S.; Schatz, G. C. Computational Simulations of the Interaction of Lipid Membranes with DNA-Functionalized Gold Nanoparticles. In *Biomedical Nanoetechnology: Methods and Protocols*; Methods in Molecular Biology *726*; Humana Press: New York, 2011; pp 283−296.

(21) Ting, C. L.; Wang, Z.-G. Interactions of a Charged Nanoparticle with a Lipid Membrane: Implications for Gene Delivery. *Biophys. J.* **2011**, *100*, 1288−1297.

(22) Vacha, R.; Martinez-Veracoechea, F. J.; Frenkel, D. Receptor-Mediated Endocytosis of Nanoparticles of Various Shapes. *Nano Lett.* **2011**, *11*, 5391−5395.

(23) Li, Y.; Li, X.; Li, Z.; Gao, H. Surface-Structure-Regulated Penetration of Nanoparticles across a Cell Membrane. *Nanoscale* **2012**, *4*, 3768−3775.

(24) Moghadam, B. Y.; Hou, W.-C.; Corredor, C.; Westerhoff, P.; Posner, J. D. Role of Nanoparticle Surface Functionality in the Disruption of Model Cell Membranes. *Langmuir* **2012**, *28*, 16318−16236.

(25) Ding, H.-m.; Tian, W.-d.; Ma, Y.-q. Designing Nanoparticle Translocation through Membranes by Computer Simulations. *ACS Nano* **2012**, *6*, 1230−1238.

(26) Werner, M.; Sommer, J. U.; Baulin, V. A. Homo-Polymers with Balanced Hydrophobicity Translocate through Lipid Bilayers and Enhance Local Solvent Permeability. *Soft Matter* **2012**, *8*, 11714−11722.

(27) Jackson, A. M.; Myerson, J. W.; Stellacci, F. Spontaneous Assembly of Subnanometre-Ordered Domains in the Ligand Shell of Monolayer-Protected Nanoparticles. *Nat. Mater.* **2004**, *3*, 330−336.

(28) Verma, A.; Uzun, O.; Hu, Y. H.; Hu, Y.; Han, H. S.; Watson, N.; Chen, S. L.; Irvine, D. J.; Stellacci, F. Surface-Structure-Regulated Cell-Membrane Penetration by Monolayer-Protected Nanoparticles. *Nat. Mater.* **2008**, *7*, 588−595.

(29) Verma, A.; Stellacci, F. Effect of Surface Properties on Nanoparticle-Cell Interactions. *Small* **2010**, *6*, 12−21.

(30) Cesbron, Y.; Shaw, C. P.; Birchall, J. P.; Free, P.; Lévy, R. Stripy Nanoparticles Revisited. *Small* **2012**, *8*, 3714−3719.
(31) Pogodin, S.; Slater, N. K. H.; Baulin, V. A. Surface Patterning of Carbon Nanotubes Can Enhance Their Penetration through a Phospholipid Bilayer. *ACS Nano* **2011**, *5*, 1141−1146.
(32) Ramalho, J. P. P.; Gkeka, P.; Sarkisov, L. Structure and Phase Transformations of Dppc Lipid Bilayers in the Presence of Nanoparticles: Insights from Coarse-Grained Molecular Dynamics Simulations. *Langmuir* **2011**, *27*, 3723−3730.
(33) Gkeka, P.; Angelikopoulos, P. The Role of Patterned Hydrophilic Domains in Nanoparticle-Membrane Interactions. *Curr. Nanosci.* **2011**, *7*, 690−698.
(34) Monticelli, L.; Kandasamy, S. K.; Periole, X.; Larson, R. G.; Tieleman, D. P.; Marrink, S. J. The Martini Coarse-Grained Force Field: Extension to Proteins. *J. Chem. Theory Comput.* **2008**, *4*, 819−834.
(35) Torrie, G. M.; Valleau, J. P. Non-Physical Sampling Distributions in Monte-Carlo Free-Energy Estimation - Umbrella Sampling. *J. Comput. Phys.* **1977**, *23*, 187−199.
(36) Kumar, S.; Bouzida, D.; Swendsen, R. H.; Kollman, P. A.; Rosenberg, J. M. The Weighted Histogram Analysis Method for Free-Energy Calculations on Biomolecules 0.1. The Method. *J. Comput. Chem.* **1992**, *13*, 1011−1021.
(37) Kumar, S.; Rosenberg, J. M.; Bouzida, D.; Swendsen, R. H.; Kollman, P. A. Multidimensional Free-Energy Calculations Using the Weighted Histogram Analysis Method. *J. Comput. Chem.* **1995**, *16*, 1339−1350.
(38) Berberich, E.; Fogel, E.; Halperin, D.; Kerber, M.; Setter, O. Arrangements on Parametric Surfaces II: Concretizations and Applications. *Math. Comput. Sci.* **2010**, *4*, 67−91.
(39) Berendsen, H. J. C.; Marrink, S. J. Molecular-Dynamics of Water Transport through Membranes - Water from Solvent to Solute. *Pure Appl. Chem.* **1993**, *65*, 2513−2520.
(40) Marrink, S. J.; Berendsen, H. J. C. Simulation of Water Transport through a Lipid-Membrane. *J. Phys. Chem.* **1994**, *98*, 4155−4168.
(41) Mills, T. T.; Toombes, G. E. S.; Tristram-Nagle, S.; Smilgies, D. M.; Feigenson, G. W.; Nagle, J. F. Order Parameters and Areas in Fluid-Phase Oriented Lipid Membranes Using Wide Angle X-ray Scattering. *Biophys. J.* **2008**, *95*, 669−681.
(42) Erber, T.; Hockney, G. M. Equilibrium-Configurations of N Equal Charges on a Sphere. *J. Phys. A: Math. Gen.* **1991**, *24*, L1369−L1377.
(43) Glasser, L.; Every, A. G. Energies and Spacings of Point Charges on a Sphere. *J. Phys. A: Math. Gen.* **1992**, *25*, 2473−2482.
(44) Thomson, J. J. On the Structure of the Atom: An Investigation of the Stability and Periods of Oscillation of a Number of Corpuscles Arranged at Equal Intervals around the Circumference of a Circle; with Application of the Results to the Theory of Atomic Structure. *Philos. Mag.* **1904**, *7*, 237−265.
(45) Singh, C.; Ghorai, P. K.; Horsch, M. A.; Jackson, A. M.; Larson, R. G.; Stellacci, F.; Glotzer, S. C. Entropy-Mediated Patterning of Surfactant-Coated Nanoparticles and Surfaces. *Phys. Rev. Lett.* **2007**, *99*, 4.